Journal of Materials Chemistry C

PAPER

View Article Online
View Journal | View Issue

Cite this: J. Mater. Chem. C, 2014, 2, 1141

Large cyano- and triazine-substituted D–π–A–π–D structures as efficient AIEE solid emitters with large two-photon absorption cross sections†

Wei Huang,[a] Fansheng Tang,[a] Bo Li,[b] Jianhua Su[a] and He Tian*[a]

Received 29th September 2013
Accepted 25th October 2013

DOI: 10.1039/c3tc31913j

www.rsc.org/MaterialsC

A series of new large π-conjugated molecules including diphenylamine and carbazole have been synthesized and characterized (**3a–c**). All compounds display aggregation-induced emission enhancement (AIEE) characteristics: exhibiting weak fluorescence in pure THF, while a significant AIEE effect is observed in mixtures with a water fraction (f_w) of 90% with a sharp increase in fluorescence intensity. Combining intramolecular charge transfer (ICT) characteristics and AIEE features, **3a–c** are intense solid emitters (589 nm, 546 nm and 556 nm, respectively) with high quantum efficiencies of 18.1%, 27.4% and 14.9%, respectively. Their two-photon absorption (2PA) properties have been investigated using the open-aperture *Z*-scan technique, and the values of the 2PA cross section at 800 nm for **3a–c** are 1363 GM, 413 GM and 5782 GM, respectively. Their excellent 2PA properties and solid quantum efficiencies pave the way for their potential use in biophotonic and optoelectronic applications.

Introduction

Organic materials displaying a large two-photon absorption (2PA) have drawn much attention in recent years, owing to their potential application in two-photon dynamic therapy, up-converted lasing,[1] power limiting materials[2] and so forth. To realize their full potential application, a series of new compounds with large 2PA cross sections (σ) have been investigated both experimentally and theoretically. Due to the research efforts of scientists, the structure of molecules with intramolecular charge transfer from donor groups to a π-bridge can improve the 2PA cross sections.[3] The molecular designs include symmetrical donor–π-bridge–acceptor (D–π–A), donor–π-bridge–donor (D–π–D) and donor–π-bridge–acceptor–π-bridge–acceptor–π-bridge–donor (D–π–A–π–A–π–D).[4] Other factors such as solvent polarity, molecular planarity, and hydrogen-bonding can also enhance the 2PA cross sections.[5]

However, highly efficient 2PA materials have suffered from low fluorescence efficiency in aqueous media, which greatly limits their biophotonic applications. It is necessary for the 2PA dyes to be soluble or dispersible in water and remain highly fluorescent in aqueous media.[6] Most 2PA molecules are soluble in organic solvents, but they lose their fluorescence in aqueous media, due to self-aggregation driven by limited solubility as well as π–π interactions. To solve this problem, Tang and co-workers found an exciting phenomenon that could overcome fluorescence quenching in aggregation, which is called aggregation-induced emission (AIE).[7] They found that the phenomenon was caused by restricted intramolecular vibrational and rotational motions (RIR) in the aggregated solid.[8] In view of this, some special 2PA dyes which had a large two-photon activity and were able to overcome fluorescence quenching in aggregation were designed and synthesized. Prasad and co-workers have synthesized a dye with aggregation-enhanced fluorescence and two-photon absorption in nano-aggregates by hindering molecular internal rotations.[9] Tang and coworkers also discovered luminogenic molecules and polymers displaying 2PA and AIE properties, based on tetraphenylethene.[3] Yang found several molecules using anthracene as the π-center with excellent 2PA and AIEE properties.[10] Li *et al.* have prepared a series of compounds based on carbazole with AIE properties as well.[11]

Triphenylamine and carbazole were widely used in electroactive materials, because they have good electron-donating and transporting capabilities, as well as a special propeller starburst molecular structure.[12] Recently, 2PA materials with triphenylamine and carbazole as electron-donors have attracted much attention. We also added *tert*-butyl to the carbazole to solve the issue of compound solubility and enhance the electron-donation. On the other hand, cyano-substituted compounds and 1,3,5-triazine-based compounds show good optical and electrical properties due to their high electron affinities and symmetrical structures.[13,14] Molecules using the cyano group and the triazine group as electron-accepting centers linked through a π-bridge have shown excellent 2PA properties.[15] In

[a]Key Laboratory for Advanced Materials and Institute of Fine Chemicals, East China University of Science & Technology, Shanghai, 200237, China. E-mail: tianhe@ecust.edu.cn; Fax: +86-21-64252756; Tel: +86-21-64252756

[b]Key Laboratory of Polar Materials and Devices, Ministry of Education, East China Normal University, Shanghai 200241, China

† Electronic supplementary information (ESI) available. See DOI: 10.1039/c3tc31913j

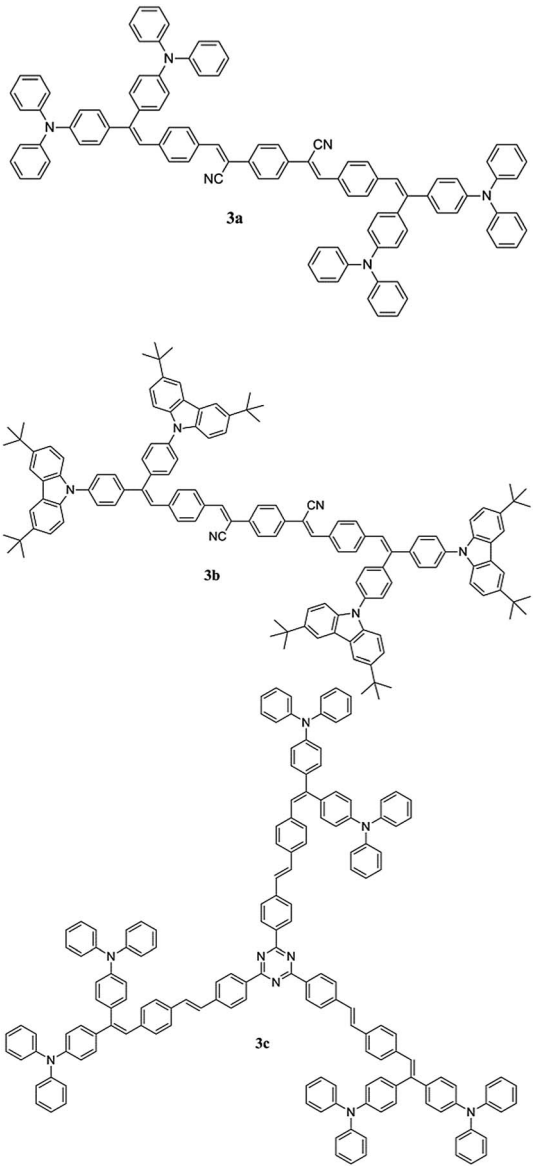

Scheme 1 Molecular structures of **3a–c**.

this work, we have synthesized three new types of D–π–A–π–D compound by using diphenylamine and carbazole groups as electron-donors and cyano and triazine groups as electron-acceptors (**3a–c**). It could be expected that the compounds with a multi-branched structure containing multi-electron donating end capping groups should have excellent 2PA values as well as AIE and AIEE properties (Scheme 1).

Results and discussion

Synthesis

The synthetic routes of the three compounds, **3a–c**, are shown in Scheme 2. The molecules were prepared by the Wittig reaction and Knoevenagel condensation.[16,17] All of the final compounds were confirmed by proton and carbon nuclear magnetic resonance spectroscopy (^{1}H NMR, ^{13}C NMR) and

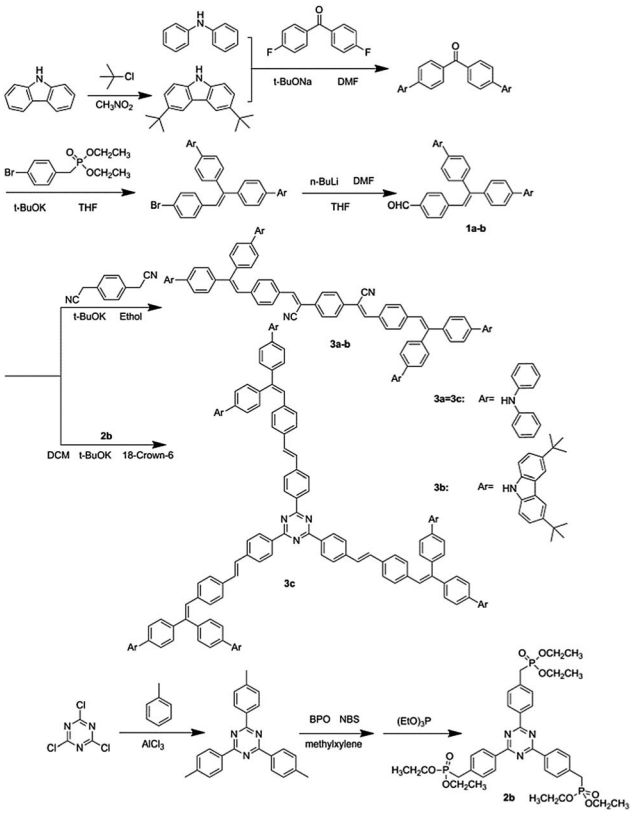

Scheme 2 Synthetic routes of compounds **3a–c**.

matrix-assisted laser desorption/ionization–time of flight mass spectroscopy (MALDI-TOF).

One-photon absorption

The normalized one-photon absorption spectra of these compounds in THF are displayed in Fig. 1. All of the dyes exhibit intense linear absorption in the UV/Vis region, and the peak wavelengths of the compounds are at 457 nm (**3a**), 420 nm (**3b**), and 418 nm (**3c**). It is clearly shown that the peak of **3a** is red shifted by 37 nm and 39 nm compared to that of **3b** and **c**,

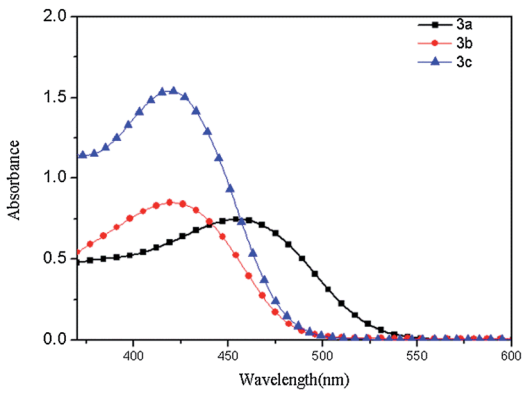

Fig. 1 One-photon absorption of **3a–c** in THF with a concentration of 1×10^{-5} M.

respectively, which supports the fact that the diphenylamine unit is a stronger electron-donor than carbazole and cyano is a stronger electron-acceptor than triazine. So the intramolecular charge transfer (ICT) of **3a** is the largest of these compounds.

Solvent effect

The solvent effect is usually observed for molecules with a D–π–A structure. The solvent effect behaviour was investigated to evaluate the effect of the solvent polarity on the compounds (Fig. 2a–c). The emission spectra of **3a–c** were recorded in different solvents by increasing the polarity from cyclohexane to *N*,*N*-dimethylformamide (DMF). A positive solvent effect was observed in **3a–c**. For example, for **3a** the emission peak at 548 nm in cyclohexane undergoes a bathochromic shift to 646 nm in DMF. A similar phenomenon is observed for **3b** and **c**. These results indicate that a significant ICT effect exists in these compounds.

AIEE properties

To investigate the AIEE attributes of **3a–c**, we used anhydrous THF as the good solvent and water as the poor solvent. The dispersions of nano-aggregates of **3a–c** were prepared by the precipitation method, adding different amounts of water to the pure THF solutions and defining the water fraction (f_w) at 0–90%. Fig. 3a shows the corresponding emission spectra of **3a** at a concentration of 1×10^{-5} M. When $f_w < 50\%$, the PL intensity of **3a** doesn't increase and is almost weak, but it increases dramatically when $f_w > 50\%$. When $f_w = 90\%$, the photoluminescence (PL) intensity is boosted to the maximum. Apparently, the emission of **3a** is induced by aggregation, thus verifying its AIEE nature. In the pure solvent, rotations of the diphenylamine peripheries against the benzene core may effectively deactivate its excited state to non-radiative, resulting in low emission from the dye. Restricting the intramolecular rotations in the aggregates blocks the non-radiative decay path and activates the radiative decay, hence changing the dye to a strong emitter.[18]

Moreover, the strong and blue-shifted emissions of the aggregates, compared to the dyes in the solution, are possibly due to the dye crystallization in the solid film.[19] Fig. 3c shows the absorption of **3a** in solution and aggregation. In contrast to the fluorescence, the absorption spectra of **3a** was red-shifted and broadened, due to the nano-aggregated structure of the molecule. A quantitative picture of the AIEE process can be made by measuring the change of the integrands of the PL spectra with the different values of f_w.[20] As for **3a**, there was very low PL intensity when the $f_w < 50\%$, but it increased swiftly when more water was added. When the $f_w = 90\%$, the intensity reaches its highest value, with a 9-fold increase (Fig. 3b). Fig. 4a shows the scanning electron microscopy (SEM) image of compound **3a**. It revealed that a nano-aggregated structure of the dye had formed in the mixtures with a high water content.

A similar phenomenon is observed for **3b** and **c**. The PL intensity is weak in pure THF, but when the water fraction reaches 90% it gives a strong luminescence with a 5-fold and 16–fold increase in the I/I_0 ratio, respectively (Fig. 3e and i), which means that there is an increase in nano-aggregates. All of the compounds show AIEE performance, in which they exhibit strongly enhanced red and yellow fluorescence emissions.

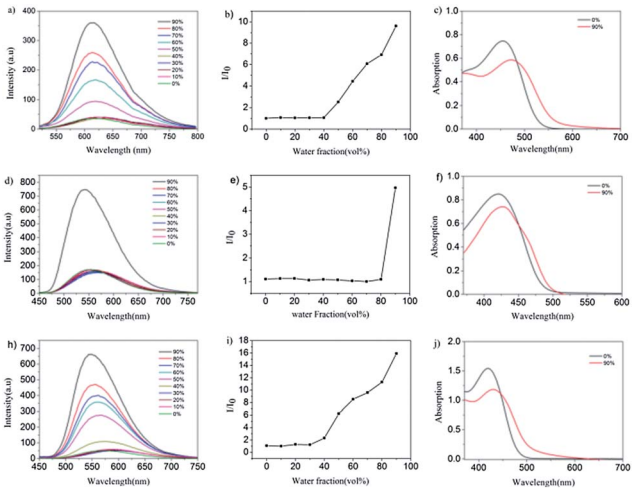

Fig. 3 (a, d and h) The PL spectra of **3a–c**, in different water fractions (f_w). (b, e and i) Plots of (I/I_0) values *versus* water content of the solvent mixture for **3a–c**. (c, f and j) Absorptions of **3a–c** in THF and water where $f_w = 90\%$ at a concentration of 1×10^{-5} M.

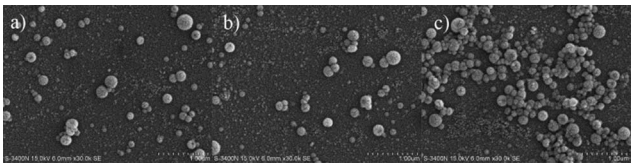

Fig. 4 (a–c) SEM images of **3a–c** nano-aggregates prepared in $f_w = 90\%$ at concentrations of 1×10^{-5} M, respectively.

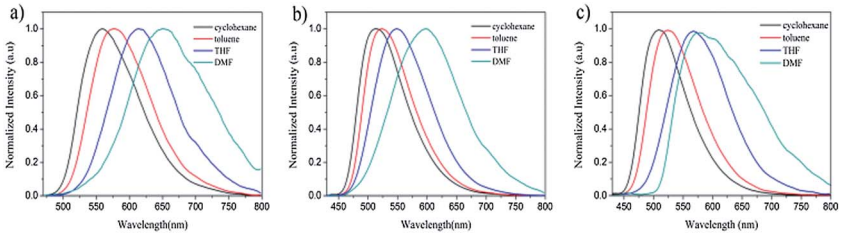

Fig. 2 (a–c) The emission spectra of **3a–c** in different solvents at the concentration of 1×10^{-5} M.

Optical properties of the solids

Such an AIEE attribute is also confirmed by the vivid images of the solid powders, (Fig. 5), where the colours of the emission are bright. The solid powders were recrystallized using toluene. To quantitatively evaluate the AIEE effect of the fluorescent materials, the emission spectra and quantum efficiencies (Φ_F) of the solid powders were measured. All of the dyes (**3a–c**) exhibited intense emission peaks at 589 nm, 546 nm and 556 nm, respectively. The Φ_F values were determined to be 18.1%, 27.4% and 14.9% for **3a–c**. We also investigated the Φ_F of **3a–c** in THF, the values were determined to be 1.5%, 5.8% and 1.4%, respectively. Such high Φ_F values of the solids indicate that they have great prospects in OLED applications.[21]

Two-photon absorption properties

The 2PA cross sections of **3a–c** were determined according to a method described previously, by using a femtosecond open-aperture *Z*-scan technique.[28] Fig. 6a, c and e show the data fitting of the open-aperture *Z*-scan.[22] The 2PA cross section σ was calculated by using the equation $\sigma = h\nu\beta/N_0$, where $N_0 = N_A C$ is the number density of absorption centers, N_A is the Avogadro constant, and C is the concentration of the solution.[23] The values of the 2PA cross section for **3a–c** are 1363 GM, 413 GM and 5782 GM, respectively, at the wavelength of 800 nm. These values are higher than those of materials previously reported, which is attributed to the large π-conjugated system and the enhanced intramolecular charge transfer (ICT) from the donor to the acceptor.[24]

The 2PA cross section of **3a** is larger than **3b**, due to the larger electron-donating strength of diphenylamine compared to that of carbazole. The 2PA value of **3c** is much larger than others. This phenomenon is due to the larger π-conjugated system of **3c**, which is in agreement with the general conclusion that enhancing the π-conjugated system could increase the value of 2PA.[25] The starburst structure of **3c** is also advantageous for the 2PA value. Therefore, we can modulate the value of the 2PA cross sections of the functional materials by simply introducing different donors and acceptors and considering the shape of molecular structure. The aggregation effect on the two-photon activity was examined by comparing the two-photon fluorescence (TPF) intensity.

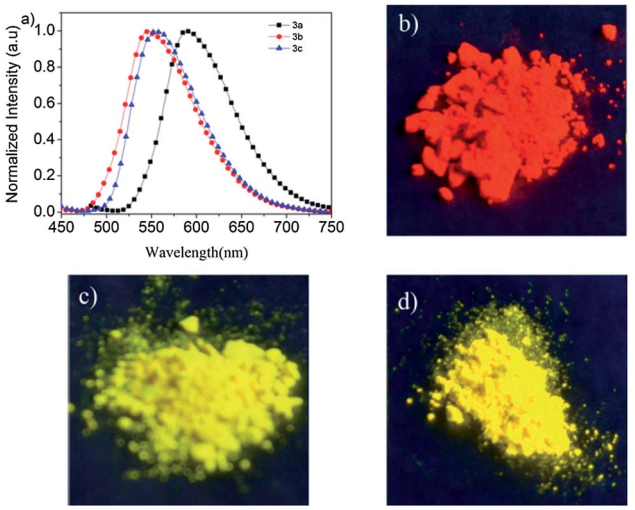

Fig. 5 (a) The normalized emission spectra of the solid powders of **3a–c**. (b–d) Images of **3a–c**, respectively, as solid powders under 365 nm light illumination.

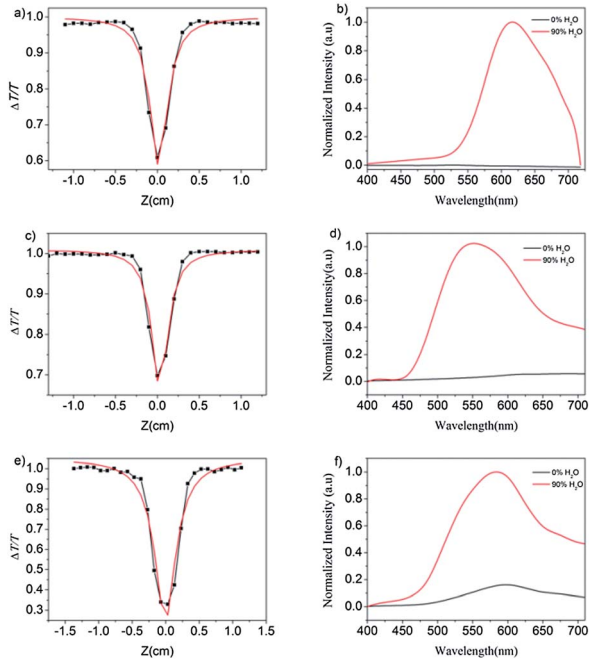

Fig. 6 (a, c and e) Open-aperture *Z*-scan trace of **3a–c** (scattered squares = experimental data, red line = theoretical fitted data). (b, d and f) The TPF emission spectra of **3a–c** in the solution ($f_w = 90\%$) at a concentration of 1×10^{-5} M.

3a–c emit intense red, yellow and deep yellow fluorescence with peaks located at 616 nm, 549 nm and 584 nm, respectively (see Fig. 6b, d and f), in a mixture of THF and water ($f_w = 90\%$), under the excitation of an 80 fs, 800 nm pulse. The good overlap between the one- and two-photon excitation fluorescence indicates that the emissions resulted from the same excited state, regardless of the mode of excitation. Fig. 7a–c show the two-photon emission images in different water fractions (f_w) of solution. No emission is observed in THF, while in the solutions where the $f_w = 90\%$ the dyes irradiate a red, yellow and deep yellow emission, when excited at 800 nm. The same phenomenon has been seen in normal emission images (Fig. 7d–f). Due to the limitation of our laser apparatus, only irradiation at the wavelength of 800 nm was used to carry out the two-photon excitation experiment. The 2PA cross sections for **3a–c** would be better in other wavelengths.[26]

Electrochemical properties

The electrochemical properties of **3a–c** are investigated by cyclic voltammetry in DCM (0.1 M solution of $(Bu_4N)PF_6$) with a saturated calomel electrode (SCE) as the reference electrode (the ferrocene/ferrocenium (Fc/Fc^+) redox couple as the external

Fig. 7 (a–c) The TPF emission images of **3a–c**, respectively, in pure THF and in a 90 : 10 water–THF mixture. (d–f) The one-photon fluorescence (OPF) emission photos of 1×10^{-5} M of **3a–c**, respectively, in different ratios of water and THF.

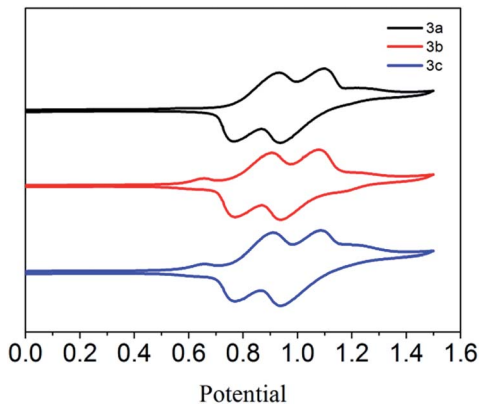

Fig. 8 Cyclic voltammograms of **3a–c** in DCM with 0.1 mol L^{-1} tetrabutylammonium hexafluorophosphate ($(Bu_4N)PF_6$).

standard), a platinum-button working electrode, and a platinum-wire counter electrode, as shown in Fig. 8. The onset oxidation potentials ($E_{onset\text{-}ox}$) for **3a–c** are 0.84 eV, 0.82 eV and 0.83 eV, respectively, giving corresponding HOMO levels for the luminogens of −5.54 eV, −5.52 eV, and −5.55 eV, respectively. The band gaps of **3a–c** can be determined from their onset absorption wavelengths and are calculated to be 2.35 eV, 2.55 eV, and 2.57 eV, respectively, giving corresponding LUMO levels for the luminogens of −3.19 eV, −2.95 eV, and −2.98 eV, respectively. The energy level parameters of **3a–c** are listed in Table 1.

Table 1 Electrochemical and optical properties of **3a–c**[a]

Compound	$E_{onset\text{-}ox}$ (v)	HOMO (eV)	λ_{onset} (nm)	E_g (eV)	LUMO (eV)
3a	0.84	−5.54	522	2.35	−3.19
3b	0.82	−5.52	488	2.55	−2.95
3c	0.83	−5.55	483	2.57	−2.98

[a] Abbreviations: $E_{onset\text{-}ox}$ = onset oxidation potential measured by cyclic voltammetry, HOMO = highest occupied molecular orbital derived by the equation: HOMO = $-(E_{onset\text{-}ox} + 4.7)$ eV,[27] λ_{onset} = onset absorption wavelength, E_g = energy band gap determined form λ_{onset}, LUMO = lowest unoccupied molecular orbital = E_g + HOMO.

Conclusions

In this work, we have synthesized three molecules **3a–c**. Their AIEE properties and 2PA cross sections have been investigated, all dyes display practically weak luminescence when they are dissolved in solvents but emit intensely upon aggregate formation, demonstrating a typical AIEE feature. Respectively, the solid powders emit red, yellow and deep yellow light intensely, with solid luminescent quantum efficiencies (Φ_F) of 18.1%, 27.4% and 14.9%, due to the combined ICT and AIEE attributes. All molecules exhibit the feature of aggregation-enhanced two-photon excited fluorescence. Their values of 2PA cross section at 800 nm are 1363 GM, 413 GM and 5782 GM, respectively. Their excellent 2PA and solid quantum efficiencies pave the way for their use in biophotonic and optoelectronic applications.

Experimental section

Instruments

^1H and ^{13}C NMR spectra were measured on a Bruker AM-400 spectrometer using d-chloroform as a solvent and tetramethylsilane (TMS, $\delta = 0$ ppm) as an internal standard. The UV/Vis spectra were recorded on a Nicolet CARY 100 spectrophotometer. The PL spectra were taken on a Varian-Cary fluorescence spectrophotometer. The quantum yields of the solid powders were measured using a Quanta-φ F-3029 Integrating Sphere. The 2PA cross sections were measured by a femtosecond open-aperture *Z*-scan technique according to a previously described method. The TPF was achieved using femtosecond pulses with different intensities at a wavelength of 800 nm. The repetition rate of the laser pulses was 250 kHz and the pulse duration was 80 fs. The cyclic voltammograms of **3a–c** were obtained using a Versastat II electrochemical workstation.

Materials

THF was pre-dried over sodium for 24 h and then redistilled under an argon atmosphere from sodium benzophenone ketyl prior to use. DMF was refluxed with calcium hydride and distilled before use. Starting materials bis(4-fluorophenyl) methanone and diphenylamine were obtained from commercial sources (J&K, Aldrich), and used without further purification. The key intermediate compounds were prepared according to the previous published procedures.[29]

3,6-Di-*tert*-butyl-9*H*-carbazole. In a three-neck flask, 5 g (0.03 mol) carbazole is dissolved in 120 mL nitromethane and 8.33 g (0.09 mol) *tert*-butylchloride is slowly added dropwise under a N_2 atmosphere. This is stirred for 8 h at room

temperature and then poured into 200 mL water. The mixture was extracted with DCM (70 mL × 3). The combined organic layer was washed with water and was dried over anhydrous $MgSO_4$ and concentrated using a rotary evaporator. The residue was purified by column chromatography on silica (petroleum ether–CH_2Cl_2 = 10 : 1 v/v) to give a white solid, 6.37 g. Yield: 76%; ^{1}H NMR (400 MHz, $CDCl_3$, TMS) δ 8.1 (s, 2H), 7.46 (dd, J = 8.5, 1.9 Hz, 2H), 7.33 (d, J = 8.5 Hz, 2H), 1.55 (s, 18H).

Bis(4-(diphenylamino)phenyl)methanone. In a three-neck flask diphenylamine 6.2 g (36.7 mmol) and sodium *tert*-butoxide 5.28 g (55 mmol) are dissolved into 100 mL anhydrous DMF, then bis(4-fluorophenyl) methanone 4 g (18.3 mmol) in 50 mL anhydrous DMF solution was slowly added dropwise in 1 h under a N_2 atmosphere. The reaction mixture was refluxed for 10 h. Upon cooling, the mixture was poured into 200 mL ice water, then a deep yellow solid precipitate was filtered off and washed with ethanol. After vacuum drying 7.85 g of yellow solid was obtained. Yield: 83%; ^{1}H NMR (400 MHz, $CDCl_3$, TMS), δ: 7.74 (m, 4H), 7.35 (m, 8H), 7.22 (m, 8H), 7.14 (m, 4H), 7.02 (d, J = 8.8 Hz, 4H).

Bis(4-(3,6-di-*tert*-butyl-9*H*-carbazol-9-yl)phenyl)methanone. The compound was synthesized by the same procedure described for **1a** using bis(4-fluorophenyl)methanone and 3,6-di-*tert*-butyl-9*H*-carbazole. Yield: 83%; ^{1}H NMR (400 MHz, $CDCl_3$, TMS) δ 8.15 (d, J = 7.8 Hz, 8H), 7.78 (d, J = 8.5 Hz, 4H), 7.51 (d, J = 1.0 Hz, 8H), 1.48 (s, 36H).

4,4′-(2-(4-Bromophenyl)ethene-1,1-diyl)bis(*N*,*N*-diphenylaniline). 2 g (3.78 mmol) bis(4-(diphenylamino)phenyl)methanone was dissolved into 50 mL anhydrous THF, 1.39 g (4.52 mmol) diethyl 4-bromobenzylphosphonate was added, then 1.27 g (11.34 mmol) *t*-BuOK dissolved in 20 mL anhydrous THF was slowly added dropwise under a N_2 atmosphere at 0 °C in a ice bath. The flask was taken out of the ice bath after 30 min and stirred for 2 h at room temperature. The mixture was poured into ethanol and a white solid precipitated out. The precipitate is washed three times with ethanol and recrystallized using DCM–hexane = 1 : 20, to give a white solid 1.97 g. Yield: 78%; ^{1}H NMR (400 MHz, $CDCl_3$, TMS) δ 7.35–7.23 (m, 12H), 7.16 (d, J = 7.8 Hz, 2H), 7.13 (m, 8H), 7.01–6.90 (m, 10H), 6.78 (s, 1H).

9,9′-((2-(4-Bromophenyl)ethene-1,1-diyl)bis(4,1-phenylene))bis(3,6-di-*tert*-butyl-9*H*-carbazole). The compound was synthesized using the same procedure described above for 4,4′-(2-(4-bromophenyl)ethene-1,1-diyl)bis(*N*,*N*-diphenylaniline) using bis(4-(3,6-di-*tert*-butyl-9*H*-carbazol-9-yl) phenyl)methanone and diethyl 4-bromobenzylphosphonate. Yield: 84%; ^{1}H NMR (400 MHz, $CDCl_3$, TMS) δ 8.16 (d, J = 4.7 Hz, 4H), 7.61 (q, J = 8.6 Hz, 6H), 7.56–7.40 (m, 10H), 7.36 (d, J = 8.3 Hz, 2H), 7.09 (s, 1H), 7.03 (d, J = 8.3 Hz, 2H), 1.48 (d, J = 3.4 Hz, 36H).

4-(2,2-Bis(4-(diphenylamino)phenyl)vinyl)benzaldehyde (1a). In a 50 mL Schlenk reactor, 1.34 g (2 mmol) 4,4′-(2-(4-bromophenyl)ethene-1,1-diyl)bis(*N*,*N*-diphenylaniline) was dissolved in 30 mL anhydrous THF at −78 °C under a N_2 atmosphere. After 30 min 1 mL of 2.4 mol L^{-1} *n*-BuLi in hexane was injected. 1 h later, 0.37 g (5 mmol) anhydrous DMF was added and stirred for 2 h. Then the reactor was taken out and the mixture was stirred overnight at room temperature. The mixture was poured into water and extracted using DCM (30 mL × 3). The combined organic layer was washed with water, dried over anhydrous $MgSO_4$, and concentrated using a rotary evaporator. The residue was purified by column chromatography on silica (petroleum ether–CH_2Cl_2 = 2 : 1 v/v) to give a yellow solid 0.61 g. Yield: 71%; ^{1}H NMR (400 MHz, $CDCl_3$, TMS) δ 9.92 (s, 1H), 7.67 (d, J = 8.2 Hz, 2H), 7.32–7.24 (m, 10H), 7.21 (d, J = 8.1 Hz, 2H), 7.13 (d, J = 8.0 Hz, 8H), 7.09–6.98 (m, 10H), 6.90 (s, 1H).

4-(2,2-Bis(4-(3,6-di-*tert*-butyl-9*H*-carbazol-9-yl)phenyl)vinyl) benzaldehyde (2b). The compound was synthesized using the same procedure as described above for compound **1a**. Yield: 72%; ^{1}H NMR (400 MHz, $CDCl_3$, TMS) δ 9.21 (s, 1H) 8.24 (d, J = 4.2 Hz, 4H), 7.81 (q, J = 8.6 Hz, 6H), 7.66–7.10 (m, 12H), 7.01 (s, 1H), 6.83 (d, J = 8.3 Hz, 2H), 1.48 (d, J = 3.4 Hz, 36H).

(2*Z*,2′*Z*)-2,2′-(1,4-phenylene)bis(3-(4-(2,2-bis(4-(diphenylamino)phenyl)vinyl)phenyl)acrylonitrile) (3a). 619 mg (1 mmol) **1a** and 78 mg (0.5 mmol) 2,2′-(1,4-phenylene)diacetonitrile were dissolved in 25 mL anhydrous ethanol. 561 mg (5 mmol) *t*-BuOK was added under a N_2 atmosphere. After refluxing for 12 h, the mixture was poured into water and extracted using DCM (30 mL × 3). The combined organic layer was washed with water, dried over anhydrous $MgSO_4$ and concentrated using a rotary evaporator. The residue was purified by column chromatography on silica (petroleum ether–CH_2Cl_2 = 4 : 1 v/v) to give a red solid 420 mg. Yield: 62%; ^{1}H NMR (400 MHz, $CDCl_3$) δ 7.80–7.69 (m, 8H), 7.50 (s, 2H), 7.29–7.81 (m, 12H), 7.15 (dd, J = 16.2, 8.4 Hz, 24H), 7.09–6.99 (m, 24H), 6.90 (s, 2H). ^{13}C NMR ($CDCl_3$, 100 MHz, TMS), 109.15, 118.04, 122.63, 123.13, 123.25, 123.32, 124.68, 124.75, 125.22, 126.44, 128.56, 129.24, 129.96, 131.26, 133.50, 135.28, 136.41, 141.02, 142.16, 144.29, 147.47, 147.52, 147.55, 147.82. MALDI-TOF: [M] calcd for $C_{100}H_{72}N_6$: 1356.5818, found: 1356.5847. Anal. calcd for $C_{100}H_{72}N_6$: C, 88.46; H, 5.35; N, 6.19. Found: C, 88.28; H, 5.46; N, 5.87%.

(2*Z*,2′*Z*)-2,2′-(1,4-phenylene)bis(3-(4-(2,2-bis(4-(3,6-di-*tert*-butyl-9*H*-carbazol-9-yl)phenyl)vinyl)phenyl)acrylonitrile) (3b). The compound was synthesized using the same procedure as described above for compound **3a**. Yield: 61%; ^{1}H NMR (400 MHz, $CDCl_3$) δ 8.16 (s, 8H), 7.82 (d, J = 8.5 Hz, 4H), 7.77 (s, 4H), 7.63 (tt, J = 18.4, 9.2 Hz, 12H), 7.57–7.41 (m, 22H), 7.28 (d, J = 8.5 Hz, 4H), 7.20 (s, 2H), 1.48 (s, 72H). ^{13}C NMR ($CDCl_3$, 100 MHz, TMS), 30.99, 33.73, 108.23, 108.97, 115.28, 116.81, 122.49, 122.51, 122.63, 122.74, 125.34, 125.49, 125.95, 126.99, 128.04, 128.38, 129.15, 130.81, 131.02, 134.21, 136.99, 137.13, 137.89, 139.01, 139.94, 140.99, 142.84, 142.06, 142.26. MALDI-TOF: [M] calcd for $C_{132}H_{128}N_6$: 1797.0200 found: 1797.0248. Anal. calcd for $C_{132}H_{128}N_6$: C, 88.15; H, 4.67; N,7.17. Found: C, 87.96; H, 4.75; N, 7.01%.

2,4,6-Tri-*p*-tolyl-1,3,5-triazine. 5.34 g (0.01 mol) 2,4,6-trichloro-1,3,5-triazine and 6.67 g (0.05 mol) $AlCl_3$ were mixed with 100 mL toluene in a three-neck flask, then the mixture was refluxed for 12 h. Upon cooling the mixture was poured into water and extracted using DCM (30 mL × 3). The combined organic layer was washed with water, dried over anhydrous $MgSO_4$ and concentrated using a rotary evaporator. The residue was purified by column chromatography on silica (petroleum ether–CH_2Cl_2 = 6 : 1 v/v) to give a white solid 2.67 g. Yield: 76%; ^{1}H NMR (400 MHz, $CDCl_3$, TMS) δ 8.64 (d, J = 8.2 Hz, 6H), 7.35 (d, J = 8.1 Hz, 6H), 2.47 (s, 9H).

Hexaethyl(((1,3,5-triazine-2,4,6-triyl)tris(benzene-4,1-diyl)) tris-(methylene))tris(phosphonate) (2b). In a 100 mL round-bottom flask, 2,4,6-tri-*p*-tolyl-1,3,5-triazine 2 g (5.7 mmol), 5.34 g NBS (17.1 mmol) and BPO (0.3 g, 1.2 mmol) were dissolved in 50 mL chlorobenzene and heated at 110 °C for 8 h. The mixture was filtered and the solvent was removed under vacuum. The residue was dissolved in 10 mL triethylphosphite and refluxed for 10 h. The excess trimethyl phosphite was removed under vacuum. The residue was purified by column chromatography on silica with ethyl acetate to afford the product as a white powder 2.73 g. Yield: 63%; ^{1}H NMR (400 MHz, $CDCl_3$, TMS) δ 8.72 (d, $J = 8.0$ Hz, 6H), 7.52 (dd, $J = 8.3$, 2.2 Hz, 6H), 4.11–4.00 (m, 12H), 3.29 (d, $J = 22.1$ Hz, 6H), 1.28 (t, $J = 7.1$ Hz, 18H).

4,4′,4″,4‴,4⁗,4⁗′-((((1*E*,1′*E*,1′*E*)-((1,3,5-triazine-2,4,6-triyl) tris(benzene-4,1-diyl))tris(ethene-2,1-diyl))tris(benzene-4,1-diyl)) tris(ethene-2,1,1-triyl))hexakis(*N*,*N*-diphenylaniline) (3c). In a 250 mL flask, 618 mg (1 mmol) **1a**, 253 mg (0.33 mmol) **2b**, 168 mg (1.5 mmol) *t*-BuOK, 18-crown-6 (20 mg, 0.08 mmol), and 100 mL DCM were combined under a N_2 atmosphere. The mixture was stirred at 45 °C for 12 h. Upon cooling the mixture was poured into water and extracted with DCM (30 mL × 3). The combined organic layer was washed with water and was dried over anhydrous $MgSO_4$ and concentrated using a rotary evaporator. The residue was purified by column chromatography on silica (petroleum ether–CH_2Cl_2 = 4 : 1 v/v) to give a deep yellow solid 381 mg. Yield: 53% ^{1}H NMR (400 MHz, $CDCl_3$, TMS) δ 8.76 (d, $J = 8.4$ Hz, 6H), 8.67 (d, $J = 8.1$ Hz, 3H), 7.69 (d, $J = 8.4$ Hz, 6H), 7.39 (d, $J = 8.2$ Hz, 9H), 7.33–7.27 (m, 24H), 7.22–7.09 (m, 43H), 7.08–7.01 (m, 24H), 6.90 (s, 3H). ^{13}C NMR ($CDCl_3$, 100 MHz, TMS), 122.87, 22.99, 123.08, 123.59, 124.49, 124.61, 126.38, 126.62, 127.68, 128.35, 129.89, 130.35, 131.31, 134.19, 135.06, 135.38, 136.96, 137.91, 141.48, 142.22, 147.14, 147.42, 147.56, 147.64, 171.07. MALDI-TOF: [M] calcd for $C_{159}H_{117}N_9$: 2151.9432, found: 2151.9479. Anal. Calcd for $C_{159}H_{117}N_9$: C, 88.67; H, 5.48; N, 5.85. Found: C, 88.43; H, 5.41; N, 5.97%.

Acknowledgements

This work was supported by NSFC/China and the National Basic Research 973 Program.

Notes and references

1 (*a*) A. Mukherjee, *Appl. Phys. Lett.*, 1993, **62**, 3423; (*b*) J. D. Bhawalkar, G. S. He, C. K. Park, C. F. Zhao, G. Ruland and P. N. Prasad, *Opt. Commun.*, 1996, **124**, 33–37; (*c*) G. S. He, T. C. Lin, V. P. Tondiglia, R. Jakubiak, R. A. Vaia and T. J. Bunning, *Appl. Phys. Lett.*, 2003, **83**, 2733–2738; (*d*) H. M. Kim and B. R. Cho, *Chem. Commun.*, 2009, 153; (*e*) M. Pawlicki, H. A. Collins, R. G. Denning and H. L. Anderson, *Angew. Chem., Int. Ed.*, 2009, **48**, 3244; (*f*) C. C. Lin, M. Velusamy, H. H. Chou, J. T. Lin and P. T. Chou, *Tetrahedron*, 2010, **66**, 8629; (*g*) Y. H. Jiang, Y. C. Wang, B. Wang, J. B. Yang, N. N. He, S. X. Qian and J. L. Hua, *Chem.–Asian J.*, 2011, **6**, 157.

2 (*a*) J. E. Ehrlich, X. L. Wu, I. Y. S. Lee, Z. Y. Hu, H. Rcockel, S. R. Marder and J. W. Perry, *Opt. Lett.*, 1997, **22**, 1843–1845; (*b*) J. W. Perry, J. M. Hales, S. H. Chi, J. Y. Cho, S. Odom, Q. Zhang, S. Zheng, R. R. Schrock, T. E. O. Screen, H. L. Anderson, S. Barlow and S. R. Marder, *Polym. Prepr.*, 2008, **49**, 989–990; (*c*) T. Brixner, N. H. Damrauer, P. Niklaus and G. Gerber, *Nature*, 2001, **414**, 57–60; (*d*) Y. Qian, K. Meng, C. G. Lu, B. Lin, W. Huang and Y. P. Cui, *Dyes Pigm.*, 2009, **80**, 174–180.

3 R. R. Hu, J. L. Maldonado, M. Rodriguez, C. M. Deng, C. K. W. Jim, J. W. Y. Lam, M. M. F. Yuen, G. R. Ortiz and B. Z. Tang, *J. Mater. Chem.*, 2012, **22**, 232–240.

4 M. Albota, D. Beljonne, J. L. Brédas, J. E. Ehrlich, J. Y. Fu, A. A. Heikal, S. E. Hess, T. Kogej, M. D. Levin, S. R. Marder, D. McCord-Maughon, J. W. Perry, H. Röckel, M. Rumi, G. Subramaniam, W. W. Webb, X. L. Wu and C. Xu, *Science*, 1998, **281**, 1653–1657.

5 H. M. Kim and B. R. Cho, *Chem. Commun.*, 2009, 153.

6 P. N. Prasad, *Introduction to Biophotonics*, Wiley-Black, NY, 2003.

7 (*a*) J. Luo, Z. Xie, J. W. Y. Lam, L. Cheng, H. Chen, C. Qiu, H. S. Kwok, X. Zhan, Y. Liu, D. Zhu and B. Z. Tang, *Chem. Commun.*, 2001, 1740–1741; (*b*) Y. Liu, S. Chen, J. W. Y. Lam, F. Mahtab, H. S. Kwok and B. Z. Tang, *J. Mater. Chem.*, 2012, **22**, 5184–5189.

8 Y. Hong, J. W. Lam and B. Z. Tang, *Chem. Commun.*, 2009, 4332–4353.

9 (*a*) S. Kim, Q. D. Zheng, G. S. He, D. J. Bharali, H. E. Pudavar, A. Baev and P. N. Prasad, *Adv. Funct. Mater.*, 2006, **16**, 2317–2323; (*b*) S. Kim, T. Y. Ohulchanskyy, H. E. Pudavar, R. K. Pandey and P. N. Prasad, *J. Am. Chem. Soc.*, 2007, **129**, 2669–2675.

10 J. F. Li, T. L. Liu, M. Zheng, M. X. Sun, D. T. Zhang, H. C. Zhang, P. P. Sun, S. F. Xue and W. J. Yang, *J. Phys. Chem. C*, 2013, **117**, 8404–8410.

11 J. Huang, X. Yang, J. Y. Wang, C. Zhong, L. Wang, J. G. Qin and Z. Li, *J. Mater. Chem.*, 2012, **22**, 2478–2484.

12 (*a*) Z. J. Ning and H. Tian, *Chem. Commun.*, 2009, 5483–5495; (*b*) X. H. Zhang, Z. S. Wang, Y. Cui, N. Koumura, A. Furbe and K. Haram, *J. Phys. Chem. C*, 2009, **133**, 13409–13415.

13 B. Wang, Y. C. Wang, J. L. Hua, Y. H. Jiang, J. H. Huang, S. X. Qian and H. Tian, *Chem.–Eur. J.*, 2011, **17**, 2647–2655.

14 W. Huang, H. T. Zhou, B. Li and J. H. Su, *RSC Adv.*, 2013, **3**, 3038–3045.

15 (*a*) M. Rumi, J. E. Ehrlich, A. A. Heikal, J. W. Perry, S. Barlow, Z. Hu, D. McCord-Maughon, T. C. Paker, H. Röckel, S. Thayumanavan, S. R. Marder, D. Beljonne and J. L. Brédas, *J. Am. Chem. Soc.*, 2000, **122**, 9500–9510; (*b*) S. J. Zheng, L. Beverina, S. Barlow, E. Zojer, J. Fu, L. A. Padilha, C. Fink, O. Kwon, Y. P. Yi, Z. G. Shuai, E. W. V. Stryland, D. J. Hagan, J. L. Brédas and S. R. Marder, *Chem. Commun.*, 2007, 1372–1374.

16 G. A. Sotzing, C. A. Thomas, J. R. Reynolds and P. J. Steel, *Macromolecules*, 1998, **31**, 3750–3752.

17 S. C. Moratti, R. Cervini, A. B. Holmes, D. R. Baigent, R. H. Friend, N. C. Greenham, J. Gruner and P. J. Hamer, *Synth. Met.*, 1995, **71**, 2117–2120.

18 Y. N. Hong, J. W. Y. Lam and B. Z. Tang, *Chem. Commun.*, 2009, 4332–4353.
19 (*a*) S. Kim, Q. D. Zheng, G. S. He, D. J. Bharali, H. E. Pudavar, A. Baev and P. N. Prasad, *Adv. Funct. Mater.*, 2006, **16**, 2317–2323; (*b*) Y. Q. Dong, J. W. Y. Lam, A. J. Qin, J. X. Sun, J. Z. Liu, Z. Lin, Z. Z. Sun, H. H. Y. Sung, I. D. Williams, H. S. Kwok and B. Z. Tang, *Chem. Commun.*, 2007, 3255–3257; (*c*) Z. Y. Zhang, B. Xu, J. H. Su, L. P. Shen, Y. S. Xie and H. Tian, *Angew. Chem., Int. Ed.*, 2011, **50**, 11654–11657.
20 Y. Liu, X. T. Tao, F. Wang, J. Shi, J. Sun, W. Yu, Y. Ren, D. Zou and M. Jiang, *J. Phys. Chem. C*, 2007, **111**, 6544–6549.
21 Y. Liu, S. M. Chen, J. W. Y. Lam, P. Lu, R. T. K. Kwok, F. Mahatb, H. S. Kwok and B. Z. Tang, *Chem. Mater.*, 2011, **23**, 2536–2544.
22 J. L. Hua, B. Li, F. S. Meng, F. Ding, S. X. Qian and H. Tian, *Polymer*, 2004, **45**, 7143–7149.
23 C. Xu and W. W. Webb, *J. Opt. Soc. Am. B*, 1996, **13**, 481.
24 X. M. Wang, F. Jin, Z. G. Chen, S. Q. Liu, X. H. Wang, X. M. Duan, X. T. Tao and M. H. Jiang, *J. Phys. Chem. C*, 2011, **115**, 776.
25 P. Y. Gu, C. J. Lu, Z. J. Hu, N. J. Li, T. T. Zhao, Q. F. Xu, Q. H. Xu, J. D. Zhang and J. M. Lu, *J. Mater. Chem. C*, 2013, **1**, 2599–2606.
26 S. B. Noh, R. H. Kim, W. J. Kim, S. Kim, K. S. Lee, N. S. Cho, H. K. Shim, H. E. Pudavar and P. N. Prasad, *J. Mater. Chem.*, 2010, **20**, 7422–7429.
27 L. J. Huo, J. H. Hou, H. Y. Chen, S. Q. Zhang, Y. Jiang, T. Chen and Y. Yang, *Macromolecules*, 2009, **42**, 6564–6571.
28 G. H. He, L. S. Tan, Q. D. Zheng and P. N. Prasad, *Chem. Rev.*, 2008, **108**, 1245–1330.
29 Z. Y. Yang, Z. G. Chi, B. J. Xu, H. Y. Li, X. Q. Zhang, X. F. Li, S. W. Liu, Y. Zhang and J. R. Xu, *J. Mater. Chem.*, 2010, **20**, 7352–7359.